4124–4140 *Nucleic Acids Research, 2007, Vol. 35, No. 12* *Published online 12 June 2007*
doi:10.1093/nar/gkm412

Rad51 and Rad54 ATPase activities are both required to modulate Rad51-dsDNA filament dynamics

Xuan Li[1], Xiao-Ping Zhang[1], Jachen A. Solinger[1], Konstantin Kiianitsa[1], Xiong Yu[2], Edward H. Egelman[2] and Wolf-Dietrich Heyer[1,3,*]

[1]Section of Microbiology, University of California, Davis, CA 95616-8665, [2]Department of Biochemistry and Molecular Genetics, University of Virginia, Charlottesville, VA 22908 and [3]Section of Molecular and Cellular Biology, University of California, Davis, CA 95616-8665, USA

Received April 3, 2007; Revised May 3, 2007; Accepted May 4, 2007

ABSTRACT

Rad51 and Rad54 are key proteins that collaborate during homologous recombination. Rad51 forms a presynaptic filament with ATP and ssDNA active in homology search and DNA strand exchange, but the precise role of its ATPase activity is poorly understood. Rad54 is an ATP-dependent dsDNA motor protein that can dissociate Rad51 from dsDNA, the product complex of DNA strand exchange. Kinetic analysis of the budding yeast proteins revealed that the catalytic efficiency of the Rad54 ATPase was stimulated by partial filaments of wild-type and Rad51-K191R mutant protein on dsDNA, unambiguously demonstrating that the Rad54 ATPase activity is stimulated under these conditions. Experiments with Rad51-K191R as well as with wild-type Rad51-dsDNA filaments formed in the presence of ATP, ADP or ATP-γ-S showed that efficient Rad51 turnover from dsDNA requires both the Rad51 ATPase and the Rad54 ATPase activities. The results with Rad51-K191R mutant protein also revealed an unexpected defect in binding to DNA. Once formed, Rad51-K191R-DNA filaments appeared normal upon electron microscopic inspection, but displayed significantly increased stability. These biochemical defects in the Rad51-K191R protein could lead to deficiencies in presynapsis (filament formation) and postsynapsis (filament disassembly) *in vivo*.

INTRODUCTION

Homologous recombination (HR) is a template-dependent, high-fidelity DNA damage repair and tolerance pathway that negotiates complex DNA damage, such as double-stranded DNA breaks (DSBs), gaps, and interstrand crosslinks, as well as stalled or collapsed replication forks (1–4). Defects in HR lead to sensitivity to genotoxic agents and genomic instability (1,5).

The process of HR can be conceptually divided into three stages. In presynapsis, the lesion is processed to a single-stranded DNA (ssDNA) intermediate. *In vivo*, ssDNA is likely bound by the ssDNA-binding protein RPA, requiring mediator proteins, such as Rad52 and the Rad55-Rad57 heterodimer, to allow formation of the presynaptic filament of Rad51-ATP-ssDNA (6–9). During synapsis, the presynaptic filament mediates homology search and DNA strand invasion to form a joint molecule or D–loop (10). In postsynapsis, Rad51 is assumed to dissociate from the product heteroduplex DNA to allow DNA synthesis from the invading 3′ end. After DNA synthesis, different sub-pathways (Synthesis-Dependent Strand Annealing, DSB Repair) generate contiguous chromosomes (2).

Rad51 and Rad54 are two key proteins in HR (1). Like RecA, Rad51 forms a helical filament on DNA in the presence of ATP and catalyzes homology search and DNA strand invasion (10–13). This reaction produces heteroduplex DNA, a central recombination intermediate. DNA-binding and DNA-strand exchange activity by budding yeast Rad51 *in vitro* requires ATP-binding but not ATP hydrolysis as revealed by the analysis of mutants in the invariant lysine residue within the Walker A box (K191 in budding yeast), as well as by using slow or non-hydrolyzable ATP analogs (10,14–19). However, *in vivo* ATP hydrolysis appears to be required for protein function (20). *Saccharomyces cerevisiae* Rad51-K191R encodes a protein that can presumably bind ATP, although this was never directly demonstrated, but not hydrolyze ATP (14). The mutant protein when expressed

*To whom correspondence should be addressed. Tel: 530 752 3001; Fax: 530 752 3011; Email: wdheyer@ucdavis.edu
Present address:
Jachen A. Solinger, IFOM-FIRC Institute of Molecular Oncology, I-20139, Milano, Italy and Konstantin Kiianitsa, Fred Hutchinson Cancer Research Center, Seattle, WA 98109-1024, USA.

at native levels in haploid cells conferred severe sensitivity to IR and a DSB-repair defect (20). Similarly, the equivalent RecA mutant (RecA-K72R) cannot complement the UV sensitivity of a RecA-deficient strain (21,22). Other ATPase defective RecA mutants show less severe defects *in vivo* (23,24). When expressed at high levels, budding yeast Rad51-K191R complements the MMS- and IR-sensitivity of a Rad51-deficient strain to near completion (14,20). The importance of ATP hydrolysis for the *in vivo* function of RecA-like proteins is underlined by the dominant-negative effect exerted by the equivalent human Rad51-K133R mutant protein when expressed in mouse, chicken or human cells (25–28). The *in vitro* and *in vivo* results regarding the requirement of ATP hydrolysis for Rad51 (RecA) function present an apparent contradiction. However, *in vitro* DNA strand invasion assays typically sidestep the requirement for product release by Rad51 (or RecA), which is achieved by SDS/proteinase K treatment. Indeed, biochemical and electron microscopic analysis of the human Rad51 protein showed that Rad51-DNA complexes are stabilized under conditions that inhibit ATP hydrolysis (15,16), suggesting a need of ATP hydrolysis for Rad51 turnover from dsDNA. Also experiments with RecA protein have demonstrated the need for ATP hydrolysis to release the heteroduplex product (19). These experiments suggest that ATP hydrolysis by Rad51 is needed to enhance filament dynamics.

Rad54 protein is a member of the Swi2/Snf2 family of dsDNA-dependent ATPases (29,30) and processively translocates along the dsDNA lattice at up to 300 bp/sec (31). Deletion of the *RAD54* gene in budding yeast confers as strong a mitotic recombination defect or IR sensitivity as a deficiency in the *RAD51* gene (1,32). *In vivo* function of Rad54 protein is largely compromised in the *rad54-K341R* mutant, which encodes a mutant Rad54 protein that is defective in ATP hydrolysis (33–36). Rad51 and Rad54 act in a single molecular pathway and physically interact (37–39). Rad54 was found to stabilize Rad51-ssDNA filaments in the presynaptic phase of recombination in an ATPase-independent fashion (40–42). Rad54 also stimulates DNA strand exchange at the synaptic stage (35,43–46). The mechanism of this stimulation is not fully understood but requires the motor function of Rad54 and depends on its ATPase activity. Possible mechanisms include the sliding of the target dsDNA during homology search, opening the target dsDNA by translocating on duplex DNA, or removing Rad51 from dsDNA that inhibit Rad51-mediated DNA strand exchange (29,30). Moreover, Rad54 was demonstrated to be able to remodel nucleosomes *in vitro*, although no effect of Rad54 on nucleosome positioning during DSB repair has been identified in budding yeast (42,47–49). During postsynapsis, Rad54 was shown to enhance branch migration during DNA strand exchange (50,51), but it is unclear whether Rad54 acts as a junction-specific motor protein like RuvB in bacteria (52). Overexpression of Rad54 leads to a decrease in conversion tract length (53) not increase as predicted, if Rad54 were to drive branch migration.

Genetic analysis suggests that Rad54 acts at a step after Rad51 protein, consistent with cytological data showing that *RAD54* is not required for Rad51 focus formation (54–58). Together with data from chromatin immunoprecipitation experiments (59,60), these results suggest that the critical function of Rad54 is either during synapsis or postsynapsis but the results are not able to distinguish between both possibilities. Since Rad54 is a dsDNA motor protein that interacts with Rad51, we have focused on the interaction between Rad54 and the Rad51-dsDNA filament (61). We discovered that Rad54 remodels the Rad51-dsDNA filament, resulting in the dissociation of Rad51 from dsDNA (41). Using electron microscopic analysis, Rad54 was found to preferentially localize to one terminus of the Rad51-dsDNA filament, consistent with Rad54 translocating along dsDNA and then docking at the end of the Rad51 filament or directly binding the filament end from solution (62). These data support a model, in which Rad54 acts as a turnover factor for the Rad51-heteroduplex DNA product complex, resulting in product release by Rad51 to allow access of the DNA synthesis machinery to the invading 3′ end. This model also rationalizes significant differences between RecA and Rad51. RecA exhibits ~200-fold higher ATPase activity on dsDNA and releases from DNA after ATP hydrolysis, whereas Rad51 appears to be much less dynamic in filament assembly/disassembly (10,15,16,19). The function of Rad54 as a Rad51 turnover factor is consistent with the absence of a Rad54 homolog in bacteria, because RecA is capable of turnover using its intrinsic ATPase activity.

Here, we analyzed the roles of both the Rad51 and Rad54 ATPase activities in turnover of the Rad51-dsDNA filament. The results revealed a number of surprising features of the *S. cerevisiae* ATPase-deficient Rad51-K191R and Rad51-K191A proteins. First, unexpectedly Rad51-K191A protein bound ATP, albeit with reduced affinity, similar to human Rad51-K133A (28). Second, the Rad51-K191R mutant protein displayed a DNA binding defect. Third, once formed the Rad51-K191R-dsDNA complexes were exceptionally stable. We demonstrate that the Rad54 ATPase activity was specifically enhanced in its interaction with the Rad51-dsDNA filament. Efficient Rad51 turnover from dsDNA required both the Rad51 and Rad54 ATPase activities. These results show that Rad51 is not a passive remodeling target of Rad54 and uncovered an intricate cooperation between the Rad51 and Rad54 ATPase activities in Rad51 turnover.

MATERIALS AND METHODS

Proteins and DNA

Saccharomyces cerevisiae Rad51, Rad51-K191R and Rad51-K191A proteins were purified after overexpression in the cognate host (6,10). Rad54 protein was overexpressed as an N-terminal GST fusion, and the tag was released by PreScission protease cleavage. The overexpression of Rad54 and its initial purification by glutathione-Sepharose 4B (Pharmacia) chromatography was performed as described (35), except that the

sodium chloride concentration was changed to 500 mM. After GST-Rad54 protein was bound on the GST-column, purified PreScission protease, itself a GST fusion protein, was loaded on the column at an enzyme to substrate molar ratio of about 1:1. The column was washed with PBS buffer (140 mM NaCl, 2.7 mM KCl, 10 mM Na_2HPO_4, 1.8 mM KH_2PO_4) containing 500 mM NaCl to remove unbound protease. Cleavage of the GST-tag from GST-Rad54 was achieved by sealing the column outlet, re-suspending the matrix in buffer A [(20 mM Tris–HCl pH 7.5, 1 mM EDTA, 10% glycerol, 10 mM β-mercaptoethanol, 1 mM phenylmethanesulfonyl fluoride (PMSF, Fluka), 1 μM pepstatin A, 2 μM benzamidin and 1 μM leupeptin] containing 500 mM NaCl, and incubation for 12 h at 4°C (63). The untagged Rad54 was eluted from the column with buffer A. Fractions containing the untagged-Rad54 were pooled and applied to a hydroxylapatite (HAP) column. The HAP column was eluted by a K_2HPO_4 buffer gradient from 20 to 500 mM (containing 500 mM NaCl), at a flow rate of 0.3 ml/min. The fractions containing Rad54 protein were collected, concentrated and dialyzed to storage buffer and stored at −80°C as described (35). Single-stranded φX174 virion DNA and double-stranded φX174-RFI DNA were purchased from New England Biolabs. The 600-bp dsDNA substrate was prepared by standard PCR with φX174-RFI template using primer olWDH427 5′- TTATCGAAGCGCGCATAAAT-3′, and primer olWDH431 5′-GTCTTCATTTCCATGCGGTG-3′. The 621 nt ssDNA substrate was prepared by one-sided PCR from PstI-linearized φX174-RFI using primer olWDH431. Both DNA substrates were purified using the Qiagen gel extraction kit. Protein concentrations are given in moles of monomers, ssDNA concentrations are given in moles of nts, and dsDNA concentrations are given in moles of basepairs.

ATP binding assay

Binding was performed in 10 μl reactions in ATPase reaction buffer [25 mM triethanolamine pH 7.5, 1.8 mM DTT, 13 mM magnesium acetate and 100 μg/ml bovine serum albumin (BSA)] containing 2.0 μM Rad51, Rad51-K191R or Rad51-K191A. For each reaction, ATP from a stock solution spiked with ∼30 μCi α-^{32}P-ATP was added to the indicated final concentration. After incubating 15 min at 30°C, the reactions were placed on a piece of parafilm on top of ice and irradiated at 254 nm in a UV-crosslinker (XL-1000, Spectronics) at about 10 cm from the light source. The total exposure intensity was ∼1260 μJ/cm^2. The reactions were incubated at 100°C for 5 min, and the proteins resolved by 10% SDS–PAGE. The gels were dried, and analyzed by PhosphoImager and quantified by ImageQuant software (Molecular Dynamics, Inc., Sunnyvale, CA, USA). For the azido-ATP labeling experiments, an ATP stock solution (400 μM) was spiked with α-P^{32}-8-Azido-ATP (MP Biomedicals) to 0.36 μCi/μl, and the experiment was conducted as described above.

Salt titration of protein–DNA complexes

Salt titrations of the protein–DNA complex formation was performed by incubating Rad51 or Rad51-K191R (2 μM) with DNA (6 μM of 600- bp dsDNA or 621-nt ssDNA) in the presence of the indicated sodium chloride concentration for 15 min at 30°C. The reactions were then fixed with glutaraldehyde (0.25%). Nucleoprotein gel electrophoresis was conducted in 1% agarose in TAE buffer (40 mM Tris–Base, 20 mM acetic acid, 1 mM EDTA) for 2 h at 4 V/cm. The dried gels were analyzed by PhosphoImager and quantified using ImageQuant software (Molecular Dynamics, Inc., Sunnyvale, CA, USA). Salt titrations of the protein–DNA complex stability were performed as above but with incubation in the absence of sodium chloride for 15 min at 30°C to allow the formation of the protein–DNA complexes. Sodium chloride was then added to the indicated final concentrations, and the protein–DNA complexes were incubated for another 30 min at 30°C. The reactions were then fixed with glutaraldehyde (0.25%). Nucleoprotein gel electrophoresis and analysis was performed as described above.

ATPase activity of Rad51

ATPase assays were performed in the ATPase reaction buffer [25 mM triethanolamine (pH 7.5), 1.8 mM dithiothreitol, 13 mM magnesium acetate and 100 μg/ml BSA], with 5 mM ATP, 2.5 μM of Rad51 (or Rad51-K191R, or Rad51-K191A), with or without 30 μM of ssDNA (poly-dA), for 10 min at 30°C. By supplementing 20 U/ml lactate dehydrogenase (Sigma), and ATP regeneration system [20 U/ml pyruvate kinase (Sigma), 3 mM phosphoenolpyruvate (Sigma) and NADH (Sigma) to give an absorbance of 1.6–1.8 (about 0.2 mg/ml)], the ATP hydrolysis rates were measured by a NADH-coupling microplate photometric assay for 60 min at 30°C as described (64).

Rad54 ATPase activity

ATPase assays were performed in ATPase reaction buffer with the indicated concentrations of ATP and 6 μM supercoiled φX174-RFI DNA for 15 min at 30°C. To form sub-saturated protein–DNA filaments (1 Rad51 per 37 bp), 0.16 μM of Rad51 or Rad51-K191R was added into the reactions. To form saturated protein–DNA filaments (1:3 bp), 2 μM of Rad51 or Rad51-K191R was added. The reactions were incubated for 60 min at 30°C, with the addition of Rad54 (3.3 nM) and the ATP regeneration system (1.5 mM of phosphoenolpyruvate, 30 U/ml of pyruvate kinase, 30 U/ml of lactate dehydrogenase and 0.2 g/ml of NADH) to initiate the reaction. The absorbance data were collected using an 8453A diode array spectrophotometer equipped with UV-visible ChemStation software (Agilent). The initial rates were calculated as described (64). The calculated initial rates were fitted into the Michaelis–Menten kinetic equation by software PRISM (Graphpad).

Nucleoprotein gel assay for Rad51 dissociation from dsDNA

The protein-dsDNA complexes were assembled by incubating 1.5 μM of Rad51 or Rad51-K191R protein with

6 μM of 600 bp DNA (labeled at 5′-end) in ATPase reaction buffer supplemented with 5 mM ATP and the ATP regeneration system (20 mM phosphocreatine and 0.1 μg/μl creatine kinase), at 30°C for 15 min. The mixture was then cooled to 24°C, and Rad54 protein (0.1 μM) was added. Following brief incubation with Rad54 (1–2 min), 5-fold molar excess of unlabeled scavenger dsDNA (30 μM herring sperm DNA) was added and the incubation continued at 24°C for the indicated times. At each time point, a 10-μl aliquot was removed and fixed with 0.25% glutaraldehyde. Nucleoprotein gel electrophoresis and analysis was performed as described above.

The Rad51-dsDNA complexes were also assembled in the presence of either 20% of ADP (1 mM ADP, 4 mM ATP), 80% ADP (4 mM ADP, 1 mM ATP) or 50 μM of ATP-γ-S at 24°C for 15 min in the absence of the ATP regeneration system. Protein-complex disassembly was monitored as described above, except 50 nM Rad54 protein was used in these assays and the ATP regeneration system was added back to the reactions together with Rad54 or storage buffer.

Topological assay for Rad51 dissociation from dsDNA

The reaction was performed as described (41). Rad51 protein (7.5 μM) was bound to dsDNA (30 μM pUC19) in 10.5 μl reactions containing 30 mM Tris acetate pH 7.5, 1 mM DTT, 50 μg/ml BSA, 20 mM magnesium acetate, 20 mM ATP, 2.5 mM spermidine and an ATP regeneration system (20 mM phosphocreatine and 0.1 μg/μl creatine kinase) for 30 min at 23°C. Rad54 (0.375 μM) was added, followed after 5 min at 23°C by addition of scavenger DNA (63 μM PstI-linearized M13mp19 dsDNA). After incubation at 23°C for 2 h, 10 U of wheat germ topoisomerase I (Promega) was added, and dsDNA was allowed to be relaxed for 1 h at 23°C. Stop buffer (final concentrations 60 mM EDTA, 0.7 mg/ml proteinase K and 0.1% SDS) was added, and reactions were deproteinized for 20 min at 23°C. Two-dimensional gel electrophoresis was performed on 1.2% agarose gels at 45 V for 22 h in the first dimension (without chloroquine). The lanes were cut out of the gels and soaked in TBE buffer (89 mM Tris–Base, 89 mM boric acid, 2 mM EDTA) with 4 μg/ml chloroquine for 2 h. New 1.2% agarose gels containing 4 μg/ml chloroquine were poured for the second dimension, and electrophoresis was performed for 22 h at 65 V in TBE containing 4 μg/ml chloroquine. Gels were stained with ethidium bromide.

Electron microscopy of nucleoprotein filaments

Protein–DNA filaments were formed by incubating either Rad51 or Rad51-K191R (at a concentration of 1.5 μM) with calf thymus dsDNA (Sigma) in 25 mM Triethanolamine–HCl buffer (pH7.2) with 1.25 mM ATP and 10 mM magnesium acetate at 37°C for 15 min. The Rad51: DNA ratio was 40: 1 (w/w). Samples were applied to carbon-coated grids and stained with 2% uranyl acetate (w/v). Grids were imaged with a Tecnai 12 electron microscope operating at 80 keV with a nominal magnification of 30 000×.

RESULTS

Purification and characterization of Rad51-K191R and Rad51-K191A proteins

The Rad51 ATPase activity appears to be critical for its biological function (12,20,25–28). Yet, the purified *S. cerevisiae* Rad51-K191R (or human Rad51-K133R) protein can catalyze *in vitro* recombination similar to the wild-type proteins (14,27). Substitution of the Walker A box residue K191 to R in the *S. cerevisiae* Rad51 protein (and K133 in human Rad51) has been assumed to block ATP hydrolysis but leave ATP binding unaffected, whereas the K to A substitution is assumed to abolish ATP binding, based on previous data (17,65). These assumptions have not been experimentally tested for *S. cerevisiae* Rad51. To understand the function of ATP hydrolysis by Rad51, in particular during the disassembly of the Rad51-dsDNA product complex by Rad54, we purified Rad51-K191R and Rad51-K191A proteins from the cognate host to apparent homogeneity (Figure 1A).

In the absence of DNA substrate, wild-type Rad51 and the mutant Rad51-K191R, and Rad51-K191A proteins display a similar and very low background ATP hydrolysis rate. Addition of the poly-dA substrate to the reaction strongly stimulated the ATP hydrolysis rate by Rad51, while the ATPase activity of both Rad51-K191R and Rad51-K191A proteins remained at the background level (Figure 1B). These results are consistent with a previous report on Rad51-K191R protein (14).

We determined the apparent ATP binding affinities for the Rad51 wild-type and Rad51-K191R/A proteins using an UV-cross-linking assay (66). Wild-type budding yeast Rad51 protein displayed non-cooperative ATP binding with an apparent K_d of 8.8 μM (Figure 1C, Table 1). This value is similar to the one determined for the human Rad51 protein with ATP-γ-S (3–5 μM) (66). The Rad51-K191R protein exhibited a reduced affinity to ATP (K_d = 52.5 μM) as compared with that of wild-type (Figure 1C, Table 1). Surprisingly, Rad51-K191A protein was found to bind to ATP with similar affinity as the Rad51-K191R protein (K_d = 34.2 μM). The binding of ATP is specific, as the BSA present in the reaction was not labeled (Figure 1C). To further confirm these observations, the UV-cross-linking analysis was carried out with a photo-affinity analog of ATP, azido-ATP. The photosensitive azido group has been used as a tool to study the corresponding specific binding site for biological ligands (67). Here, we use it as an alternative to study ATP binding by Rad51 protein. The results (Figure 1E and F; Table 1) were consistent with the previous data with α-^{32}P-ATP, showing that compared with Rad51, Rad51-K191R and Rad51-K191A exhibited reduced ATP binding affinity. We note that the Rad51-K191R showed better binding to azido-ATP than to ATP, whereas the Rad51-K191A protein showed reduced binding to azido-ATP compared with ATP (Table 1). The reasons for this difference remain unknown. The decreased affinities of the mutant proteins were also observed in the presence of ssDNA (data not shown). Azido-ATP led to minimal unspecific binding to BSA (Figure 1E). Taken together, these results challenge the often-stated assumption that

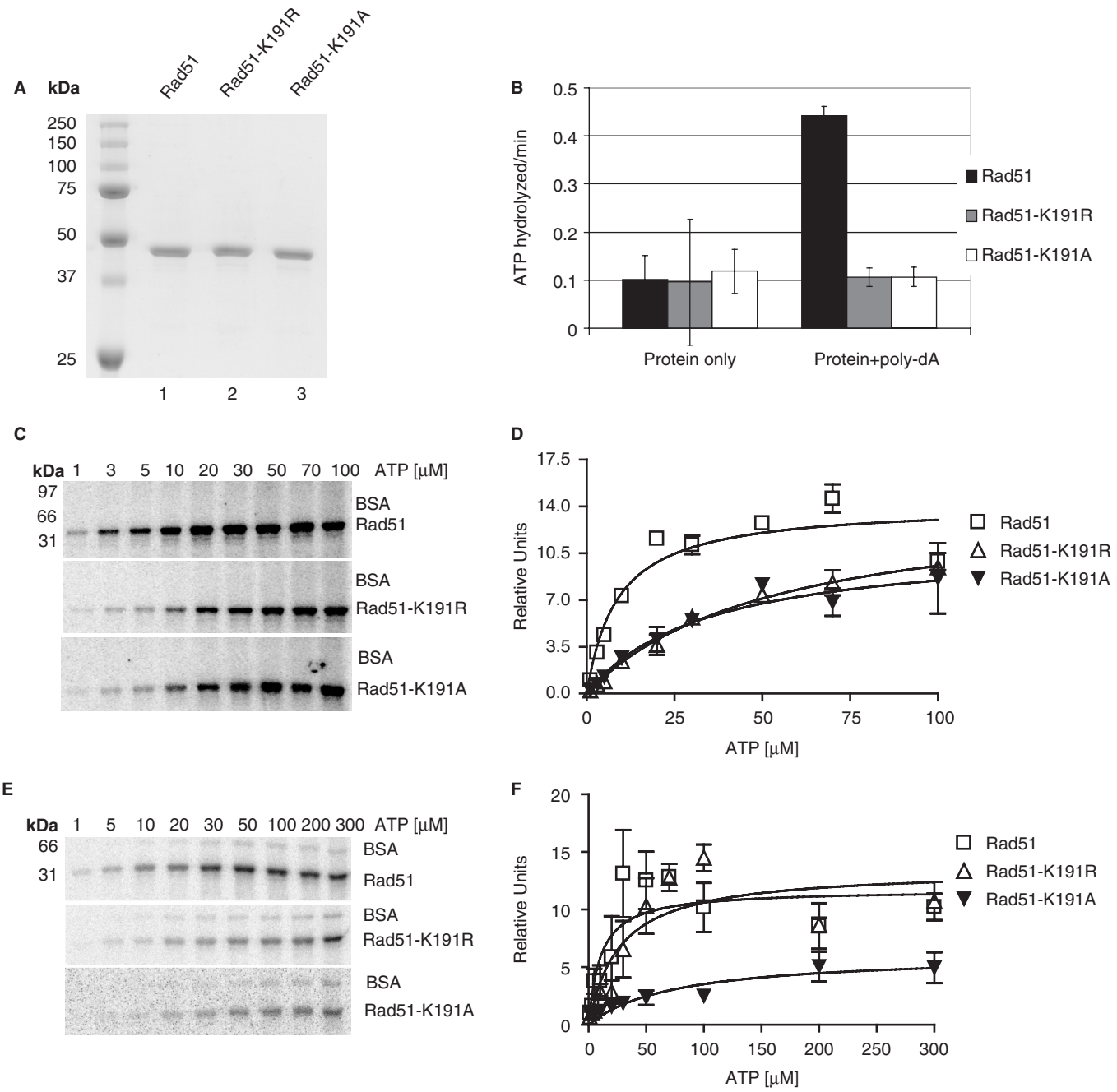

Figure 1. Purification and characterization of Rad51 proteins. (**A**) *Saccharomyces cerevisiae* Rad51 (1 μg, lane 1), Rad51-K191R (1 μg, lane 2) and Rad51-K191A (1 μg, lane 3) proteins were purified from budding yeast, analyzed by 10% SDS–PAGE and stained with Coomassie brilliant blue R250. (**B**) ATPase activity of Rad51 (dark bars), Rad51-K191R (gray bars) and Rad51-K191A (white bars) proteins. The ATPase activities of Rad51 proteins (2.5 μM) were measured either in the presence of ssDNA (30 μM, poly-dA) or absence of DNA by an NADH-coupled microplate photometric assay. ATPase activity is measured as the rate of NADH decomposition (molar molecules of NADH decomposed per minute by molar molecule of Rad51). All measurements were done in triplicate, and the error bars represent 1 SD. (**C**) α-^{32}P-ATP binding by Rad51 proteins. The Rad51-ATP complexes were resolved by 10% SDS–PAGE, and the signal intensities were quantified with a PhosphoImager. The intensity of the Rad51 band at 1 μM ATP was defined as one unit, and the signals were normalized to this standard. (**D**) Data obtained from (C) and additional gels were fitted into a saturation-binding curves using PRISM software (Graphpad). (**E**) α-P^{32}-8-Azido-ATP binding by Rad51 proteins. (**F**) Fitted saturation binding curves for data obtained from (E) and additional gels. Procedures were as in (C, D). For (C–F), the calculated K_d values are shown in Table 1. All measurements were done in triplicate and the error bars represent 1 SD. For (C, D), the positions of MW markers, BSA and the Rad51 proteins were determined by Coomassie staining and are indicated on the left and right sides.

Table 1. ATP binding

	K_d (μM) [α–P^{32}]-ATP	K_d (μM) [α-P^{32}]-8-Azido-ATP
Rad51	8.8 ± 4.5	10.2 ± 5.1
Rad51-K191R	52.5 ± 18.2	26.9 ± 10.3
Rad51-K191A	34.2 ± 25.8	73.7 ± 35.6

the lysine to alanine change in the Walker A box motif abolishes ATP binding.

Protein–DNA filament formation and stability

Both, Rad51-K191R and Rad51-K191A proteins bound DNA in a nucleotide-dependent manner (data not shown). We utilized primarily electrophoretic analysis of glutaraldehyde-fixed Rad51-DNA complexes, a method normally used with RecA (19,68) and human Rad51 (28,69). We have verified in previous studies that the electrophoretic mobility of yeast Rad51-DNA complexes corresponds within the limits of resolution to filament saturation using electron microscopy, topological assays (Figure 5), and nuclease protection assays (41,61,62). An earlier analysis failed to detect Rad51-K191A binding to DNA (44), but using fixation prior to electrophoretic analysis stabilized the Rad51-K191A-filaments sufficiently to allow their visualization (data not shown). The Rad51-K191A-dsDNA filament displayed a significant defect in its interaction with Rad54 protein. Since the purpose of the study is to understand the interaction between the Rad51 and Rad54 proteins, we focused on the Rad51-K191R protein and its interaction with Rad54 for the further analysis.

The DNA binding properties of the Rad51-K191R protein were analyzed by nucleoprotein gel assays and electron microscopy. Rad51-K191R protein formed protein–DNA filaments similar to wild-type Rad51 protein but with notable differences (Figure 2). First, we titrated increasing amounts of wild-type or Rad51-K191R proteins to a 600-bp dsDNA substrate. Consistent with a previous determination (70), Rad51 wild-type protein approached maximal binding at a stoichiometry of ~3–4 bp per Rad51 subunit in the filament (Figure 2A), as judged by the disappearance of free DNA. The Rad51-K191R protein required slightly higher protein concentrations, approaching maximal binding at a stoichiometry of 2 bp per subunit (Figure 2A). The electrophoretic mobility of the Rad51-K191R-dsDNA complexes tended to be more homogeneous than those formed by the wild-type Rad51 protein. It appeared that the Rad51-K191R protein did not form the partially saturated complexes that are evident at sub-stoichiometric amounts of wild-type Rad51 protein (Figure 2A, lanes 12 and 13). These observations suggest that the Rad51-K191R protein displays a partial dsDNA-binding defect either diminishing nucleation or enhancing binding co-operativity or both. Electron microscopic analysis of the protein–DNA complexes formed by wild-type Rad51 (Figure 2E left panel) or Rad51-K191R (Figure 2E right panel) proteins demonstrated that the Rad51-K191R mutant protein formed helical filaments on dsDNA with no discernible difference to the filaments formed by wild-type Rad51 protein.

Salt titration experiments were employed to analyze formation and stability of the protein–DNA filaments formed by either Rad51 or Rad51-K191R protein, determining the salt titration midpoints (STMs), which represent the sodium chloride concentrations at which one-half of the substrate is protein-free (71). Formation of stable Rad51-K191R-ssDNA filaments precipitously dropped at sodium chloride concentrations over 150 mM (Figure 2B, lanes 14 and 15), while the wild-type protein efficiently formed stable filaments up to about 250 mM NaCl (Figure 2B, lanes 6–8). This indicates that formation of Rad51-K191R-ssDNA filaments (STM = 228 mM) was impaired compared with that of the Rad51-ssDNA filament (STM = 305 mM) (Figure 2B and C; Table 2). In contrast, once formed, Rad51-K191R-ssDNA filaments (STM = 1900 mM) were much more stable than Rad51-ssDNA filaments (STM = 780 mM) (Figure 2C, Table 2). Rad51-ssDNA filaments disassembled completely at about 1M NaCl, while Rad51-K191R-ssDNA filaments were partially resistant up to 2 M NaCl. Like with ssDNA, the formation of Rad51-K191R-dsDNA filaments was also more sensitive to salt (STM = 78 mM) than with wild-type Rad51-dsDNA filaments (STM = 192 mM) (Figure 2D, Table 2). Rad51-K191R-dsDNA filaments were also extremely salt-resistant and remained largely intact in the presence of 2 M NaCl, while wild-type Rad51-dsDNA filaments largely disassembled (STM = 680 mM) when the concentration of sodium chloride was over 1 M (Figure 2D, Table 2).

In summary, the salt titration experiments revealed an unexpected DNA binding defect of the Rad51-K191R mutant protein and demonstrated the extraordinary stability of such complexes once formed.

ATPase activity of Rad54 in the presence of Rad51 and Rad51-K191R-dsDNA filaments

In the presence of free dsDNA substrate, Rad54 exerts a basic mode of ATPase activity, hydrolyzing about 1000 ATP per minute (61). In the presence of saturated Rad51-dsDNA filaments (3 bp/Rad51), Rad54 displays a reduced mode of ATPase activity; while in the presence of sub-saturated Rad51-dsDNA filament, Rad54 displays an enhanced mode with a 5 to 6-fold increase in ATPase activity (61). In these experiments, wild-type Rad51 protein had been utilized, leaving open the possibility that activation of the Rad51 ATPase activity contributed to the observed effect. Although the Rad51 ATPase activity is vastly lower (0.4 mol/mol/min; Figure 1B) than the ATPase activity of Rad54 (~1000 mol/mol/min), the excess of Rad51 protein in these reactions (160 nM Rad51, 3.3 nM Rad54) and the possibility that Rad51 activity is stimulated under our conditions required to control for this possibility.

We measured the kinetic parameters k_{cat} and K_M of Rad54 in the presence and absence of fully and partially saturated Rad51-dsDNA filaments. To exclude a

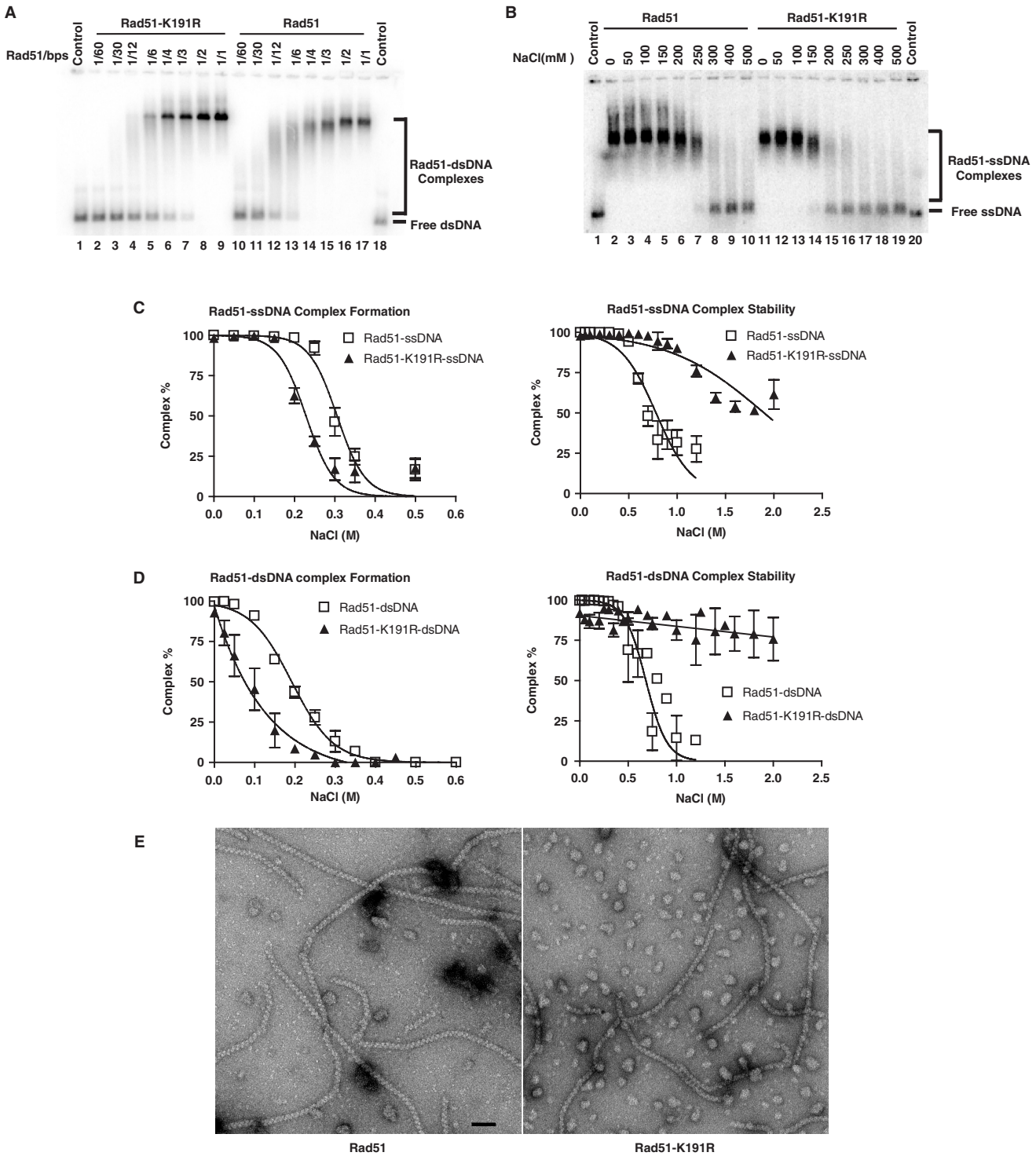

Figure 2. Rad51-DNA filament formation and stability. (**A**) Binding of Rad51 and Rad51-K191R proteins to dsDNA. Protein titration reactions were performed in ATPase reaction buffer by incubating the 600-bp DNA substrate (6 μM) with various amounts of protein (0.1, 0.2, 0.5, 1, 1.5, 2, 3, 6 μM) at 30°C for 15 min. Protein-free, labeled DNA substrate (lanes 1 and 18); Rad51 (lanes 2–9); Rad51-K191R (lanes 10–17). (**B**) Salt titration of Rad51-ssDNA and Rad51-K191R-ssDNA complex formation. The nucleoprotein complexes were assembled by incubating 2 μM of Rad51 (lanes 2–10), or Rad51-K191R (lanes 11–19) together with 6-μM ssDNA (621mer) in presence of the indicated sodium chloride concentration for 15 min at 30°C. Protein-free, labeled DNA substrate (lanes 1 and 20). (**C, D**) Quantification of the results of the Rad51 and Rad51-K191R-DNA complex formation and stability with ssDNA (C) and dsDNA (D). The data were fitted into a sigmoidal curve by PRISM software (GraphPad). All measurements were done in triplicate and the error bars represent 1 SD. The STM data calculated for these curves are shown in Table 2. (**E**) Electron micrographs of Rad51-DNA filaments formed by wild-type Rad51 (left) and Rad51-K191R mutant proteins (right). The filaments are formed on linear dsDNA in the presence of ATP. The scale bar is 500 Å.

Table 2. Salt-titration midpoints (STM) of Rad51/Rad51-K191R-DNA filaments

		STM of protein-ss DNA filament (mM)	STM of protein-ds DNA filament (mM)
Filament formation	Rad51	305 ± 11	192 ± 8
	Rad51-K191R	228 ± 13	76 ± 20
Filament stability	Rad51	$\sim 780 \pm 50$	$\sim 680 \pm 40$
	Rad51-K191R	$\sim 1900 \pm 100$	NA[a]

[a]NA,A value could not be calculated, as the filaments did not dissociate at the concentrations tested.

contribution by the Rad51 ATPase activity, the experiments were performed with both wild-type and Rad51-K191R proteins.

In the presence of sub-saturated Rad51-dsDNA filaments (1/37 bp), the ATP turnover rate of Rad54 was stimulated over 4-fold (70.5 μM/min versus 16.3 μM/min), while the ATP affinity was not significantly affected within the error of the data (482.5 μM versus 730.7 μM) (Figure 3A, Table 3). In contrast, when Rad54 was incubated with saturated Rad51-dsDNA filament (1/3 bp), the ATP turnover rate was reduced from 16.3 μM/min to 10.8 μM/min (Figure 3B, Table 3). Surprisingly, the K_M for ATP of Rad54 decreased almost 15-fold to 49.4 μM from 730.7 μM (Figure 3B, Table 3).

To formally exclude an effect of the Rad51 ATPase activity, the kinetic measurements were repeated with dsDNA filaments formed by the Rad51-K191R protein. With sub-saturated Rad51-K191R-dsDNA filaments (1/37 bp), the ATP turnover rate of Rad54 was enhanced more than 4-fold (71.1 μM/min versus 16.3 μM/min), with no significant effect on its K_M (637.9 μM versus 730.7 μM) (Figure 3A, Table 3). These values are not significantly different from those obtained with the wild-type Rad51 filaments (Table 3). With saturated Rad51-K191R-dsDNA filaments, the K_M was significantly reduced about 8-fold (93.02 μM versus 730.7 μM), similar to the experiments with wild-type Rad51. However, the ATP turnover rate was slightly stimulated (20.47 μM/min versus 16.3 μM/min) with Rad51-K191R (1/3 bp) (Figure 3B, Table 3). This latter effect differed from the wild-type Rad51 protein and is likely due to the partial DNA binding defect we observed above with Rad51-K191R. When Rad51-K191R was incubated with the dsDNA substrate at 1/3 bp stoichiometric ratio, most of the dsDNA substrate was completely covered by protein, but a small fraction of substrate remained protein-free (Figure 2A, lane 7), or possibly partially covered by protein. These substrates are likely responsible for the observed slight increase in the k_{cat}. Taken together, these results suggest that the interaction of Rad54 with subsaturated Rad51-dsDNA filaments stimulated the ATP turnover rate of Rad54, while the interaction with fully saturated Rad51-dsDNA filaments enhanced the affinity of Rad54 for ATP. While some data displayed a certain scatter, all conclusions are based on differences that are clearly significant as demonstrated by the non-overlapping errors.

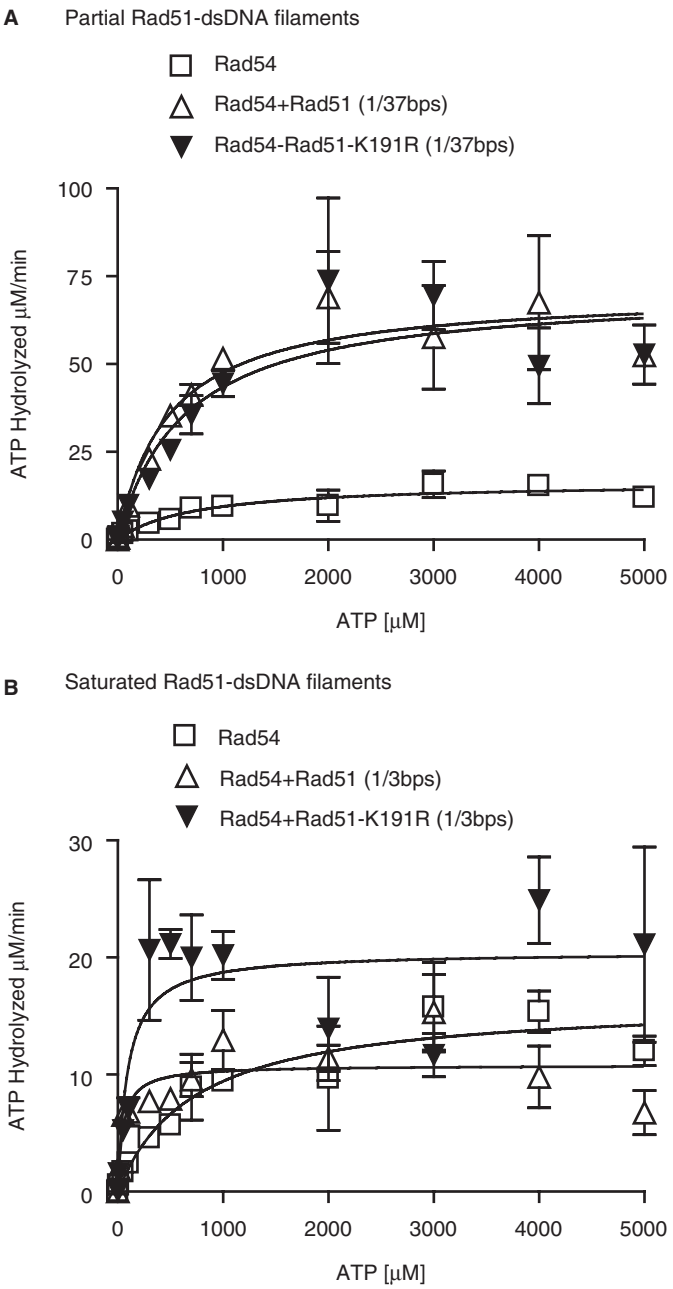

Figure 3. Rad51 and Rad51-K191R-dsDNA filaments modulate the Rad54 ATPase activity. ATPase assays were performed by incubating 3.3 nM Rad54 together with the Rad51 or Rad51-K191R-dsDNA filaments (6 μM bp) formed either at sub-saturated ratio of 1/37 bp (**A**), or at saturated ratio of 1/3 bp (**B**). For comparison, the Rad54 ATPase was also measured on protein-free dsDNA. ATPase reactions were performed under standard buffer conditions at 30°C. ATPase data were fitted into the Michaelis–Menten equation using PRISM software (Graphpad). Data points represent the average of at least three replicate experiments, and the error bars represent 1 SD. The K_M and k_{cat} values calculated for these curves are shown in Table 3.

Table 3. Kinetic data of Rad54 ATPase activity

	Rad54	Rad51 + Rad54 (1/37 bp)	Rad51 + Rad54 (1/3 bp)	Rad51-K191R + Rad54 (1/37 bp)	Rad51-K191R + Rad54 (1/3 bp)
V_{MAX} (μM/min)	16.3 ± 1.9	70.5 ± 6.3	10.8 ± 0.8	71.1 ± 34.6	20.5 ± 1.9
K_M (μM)	730.7 ± 275.4	482.5 ± 159.3	49.4 ± 26.0	637.9 ± 253.0	93.0 ± 51.1
k_{cat}/K_M ($\mu M^{-1}min^{-1}$)	6.7	43.8	65.5	33.5	66.0

Disassembly of Rad51-ATP-dsDNA filaments by Rad54

Rad54 disassembles Rad51-dsDNA filaments, and we suggested this function to be critical during postsynapsis to turnover the Rad51-heteroduplex DNA product complex (30,41). This disassembly was shown to require the Rad54 ATPase activity (41), but the requirement for the Rad51 ATPase remained unaddressed. To test a possible contribution of the Rad51 ATPase activity, we tested disassembly of Rad51-K191R-dsDNA filaments. As shown before, the Rad51-DNA filament disassembled gradually (Figure 4A, lanes 2–5). A slight accumulation of free dsDNA and reduction of the saturated filament was observed after 90 min of incubation (Figure 4A and B). Visualizing disassembly was dependent on the presence of scavenger DNA (lanes 14–17), showing that disassociated Rad51 can rebind the dsDNA. Addition of Rad54 at a sub-stoichiometric ratio (1 Rad54 per 15 Rad51) promoted nucleoprotein filament disassembly (Figure 4A, lanes 6–9). A significant accumulation of free dsDNA and reduction of the saturated filament was observed after 90 min of incubation (Figure 4A and B). Again, the presence of scavenger DNA was required, since Rad51 can rebind to dsDNA even in the presence of Rad54 (lanes 10–13). In contrast, Rad51-K191R-dsDNA filaments were extremely stable even in the presence of scavenger DNA (Figure 4C, lanes 2–5, Figure 4D), consistent with the results from the salt titrations (Figure 2D). Upon addition of Rad54, the Rad51-K191R-dsDNA filament was partially disassembled, and a gradual increase in the mobility of the nucleoprotein filament was observed during the time course (Figure 4C, lanes 6–9, Figure 4D). The presence of scavenger DNA was required to prevent Rad51-K191R to rebind the substrate (Figure 4C, lane 10–17). Furthermore, Rad54-K341R, an ATPase-deficient mutant, has no effect on either Rad51- or Rad51-K191R-dsDNA filament disassembly [(41), Figure 4D]. Together, these results suggest that the intrinsic ATPase activity of Rad51 and the ATPase activity of Rad54 are both required for the efficient turnover of Rad51 from dsDNA substrate.

Topological assay for disassembly of Rad51-ATP-dsDNA filaments by Rad54

To corroborate the results from the nucleoprotein gel assays, we employed a topological assay to examine the nucleoprotein filament disassembly (41)(Figure 5A). Rad51-dsDNA filaments partly disassembled after 2 h incubation in the presence of scavenger DNA (Figure 5B, upper left panel), indicated by the disappearance of form X DNA species and the appearance of negatively supercoiled (sc) and relaxed (re) DNA. Incubation of Rad54 with Rad51-dsDNA filament increased filament disassembly significantly, as most DNA substrate had been converted to fully relaxed DNA species after 2 h of incubation (Figure 5B). Rad51-K191R protein remained bound to the DNA substrate even in the presence of scavenger DNA, indicated by the continued presence of form X DNA after 2 h of incubation (Figure 5B). We reason that the relaxed DNA species observed in the Rad51-K191R reaction is likely to represent initially unbound DNA, because of the subtle DNA binding defect documented before (Figure 2D) rather than evidence for nucleoprotein filament disassembly. This interpretation is consistent with the absence of intermediate negatively sc DNA species. Upon incubation of Rad54 with Rad51-K191R-dsDNA filaments, the X-species disappeared and was accompanied by the appearance of a group of negative sc species, which represent partially disassembled protein–DNA filaments (Figure 5B). Taken together, the results of topological assays are consistent with the results of nucleoprotein gel assays, that the ATPase activity of Rad51 is required for efficient disassembly of Rad51-dsDNA filament by the Rad54 motor.

Disassembly of Rad51-dsDNA filament assembled with different nucleotide factors

ATP hydrolysis by Rad51 is crucial for intrinsic and Rad54-mediated nucleoprotein filament disassembly (Figures 2, 4 and 5). We tested whether the type of Rad51-bound nucleotide (ATP versus ADP) has an effect on the dissociation reaction. Rad51-dsDNA filaments containing ADP-bound subunits were assembled *in vitro*. ADP by itself cannot support the formation of Rad51-dsDNA filaments (70). Therefore, we chose to mix ADP and ATP at different ratios for efficient nucleoprotein filament assembly. Our data suggest that Rad51-dsDNA filaments can be efficiently assembled even in the presence of only 20% ATP (data not shown).

Rad51-dsDNA filaments assembled in the presence of 20% ADP were disassembled with faster kinetics than those assembled exclusively in the presence of ATP (Figure 6B, lanes 6–9, lanes 14–17, Figure 6C). Rad51-dsDNA filaments assembled in the presence of 80% ADP were disassembled even faster (Figure 6A, lanes 6–9, lanes 14–17, Figure 6C). This difference is not due to the inherent instability of Rad51-dsDNA filament assembled in the presence of ADP, since in the absence of Rad54, the amount of free DNA did not differ in reactions with 0%, 20% and 80% ADP. Rather, the filaments containing

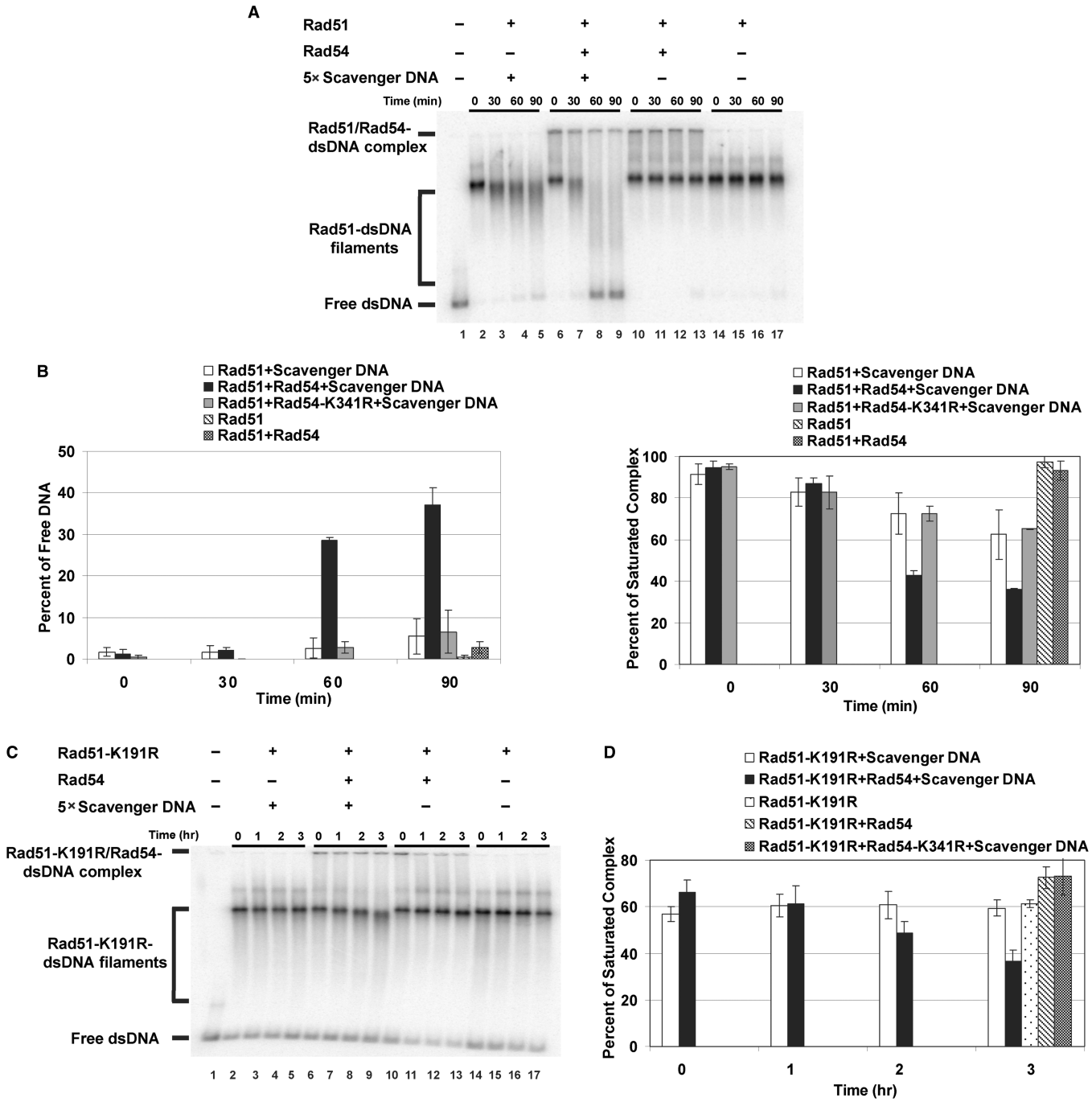

Figure 4. Both Rad51 and Rad54 ATPase activities are important for Rad51-dsDNA filament disassembly. Rad51-dsDNA filaments were formed at 4 bp/Rad51 ratio (1.5 μM Rad51, 6 μM dsDNA) for 15 min at 30°C. Initiation of Rad51-dsDNA filament disassembly was started by the addition of Rad54 (0.1 μM) and scavenger DNA (30 μM). (**A**) Protein-free, labeled DNA substrate (lane 1); Rad51-dsDNA filaments in the absence of Rad54 but with scavenger DNA (lanes 2–5), in the presence of Rad54 and scavenger DNA (lanes 6–9), in the presence of Rad54 but absence of scavenger DNA (lanes 10–13), in the absence of Rad54 and scavenger DNA (lanes 14–17). (**B**) The data from (A) and from assays where Rad54-K341R was used instead of wild-type Rad54 protein (data not shown) were quantified on a PhosphoImager. The accumulation of the band of free DNA and the reduction of lowest mobility species of the nucleoprotein filament (saturated complex) were taken as the readout of Rad51 displacement activity by Rad54, respectively. Data points represent the average of at least three replicate experiments, and error bars represent 1 SD. For the reactions with Rad51 and Rad51 + Rad54 only the 90 min data are shown. (**C**) Rad51-K191R-dsDNA filaments were formed at 4 bp/Rad51-K191R ratio (1.5 μM Rad51-K191R, 6 μM dsDNA) for 15 min at 30°C. Initiation of Rad51-K191R-dsDNA filament disassembly was started by the addition of Rad54 (0.1 μM) and scavenger DNA (30 μM). Protein-free, labeled DNA substrate (lane 1); Rad51-K191R-dsDNA filaments in the absence of Rad54 but with scavenger DNA (lanes 2–5), in the presence of Rad54 and scavenger DNA (lanes 6–9), in the presence of Rad54 but absence of scavenger DNA (lanes 10–13), in the absence of Rad54 and scavenger DNA (lanes 14–17). (**D**) The data from (C) were quantified on a PhosphoImager. The reduction of the saturated nucleoprotein filament was taken as readout of Rad51-K191R displacement by Rad54. Data points represent the average of at least three replicate experiments, and error bars represent 1 SD. For the reactions with Rad51-K191R, Rad51-K191R + Rad54 and Rad51-K191R + Rad54-K341R + scavenger DNA only the 90 min data are shown.

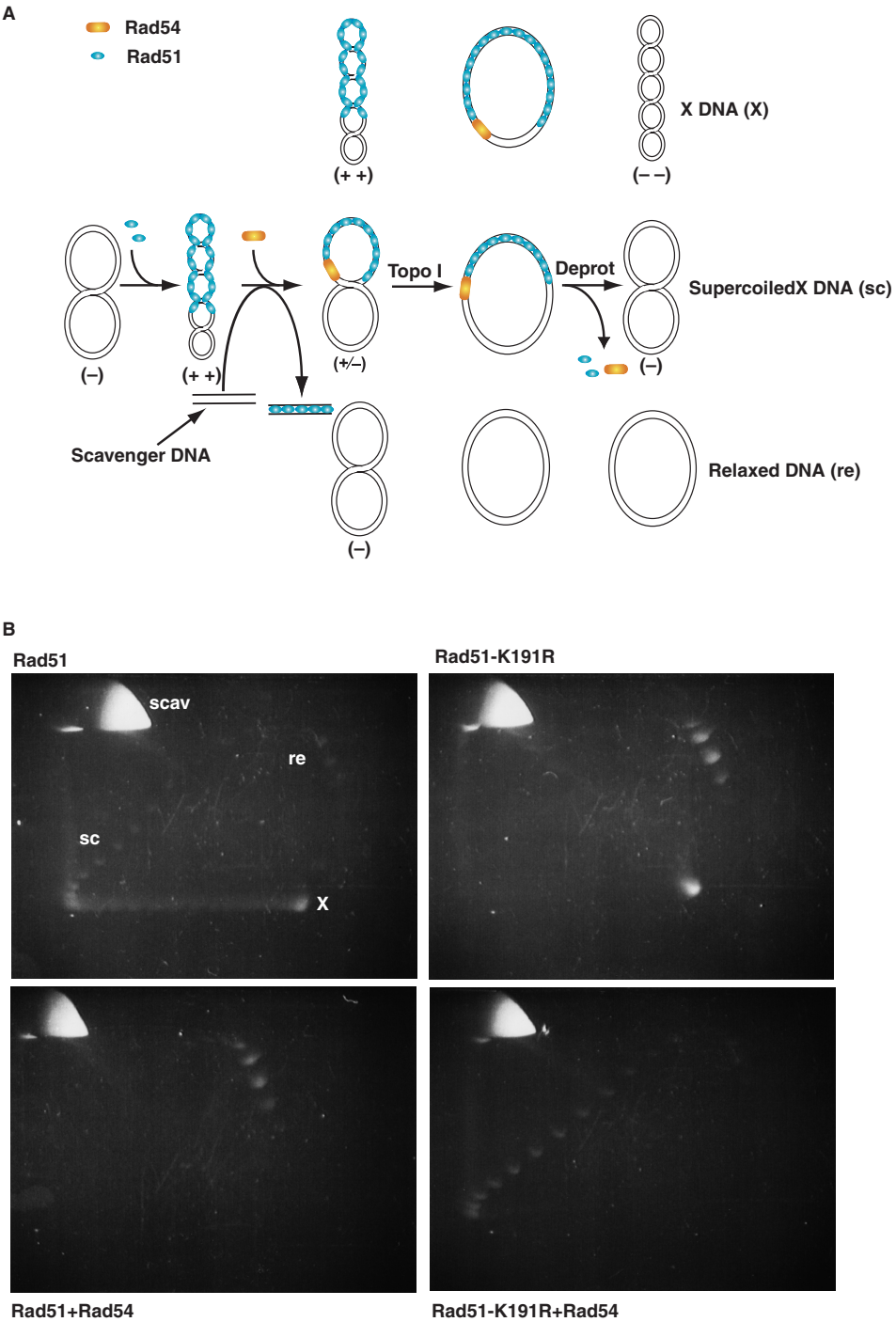

Figure 5. Topological assay of Rad51-dsDNA filament disassembly by Rad54. (**A**) Scheme of the assay. Nucleoprotein filaments were formed by incubating Rad51 or Rad51-K191R protein with the supercoiled DNA substrate. Binding by Rad51 unwinds the dsDNA and leads to the introduction of compensatory positive scs (+). Relaxation of these scs by topoisomerase I followed by deproteinization results in highly negatively supercoiled DNA, so called form X DNA (x, top). If Rad51 is completely removed from the DNA substrate by Rad54 before the treatment of topoisomerase, the substrate will be converted to a fully relaxed species (re, bottom). If Rad51 was partially removed, it will be converted to species with varying degree of negative supercoiling (x, top; sc, middle). (**B**) ATPase activity of Rad51 is important for its dissociation from dsDNA promoted by Rad54. Rad51 or Rad51-K191R (7.5 μM) was pre-incubated with pUC19 dsDNA (30 μM) for 30 min at 23°C to form nucleoprotein filaments. Rad54 (0.375 μM) was added and incubated for 5 min, followed by the addition of scavenger DNA (63 μM PstI-linearized M13mp19 dsDNA), and incubated for 2 h at 23°C. Reactions were separated on a native 1.2% agarose gel without chloroquine in the first dimension followed by a second electrophoresis step with 4 μg/ml chloroquine. The positions of supercoiled (sc), relaxed (re), X form (x) and scavenger (scav) dsDNA are indicated in the first gel for the reaction with Rad51 protein.

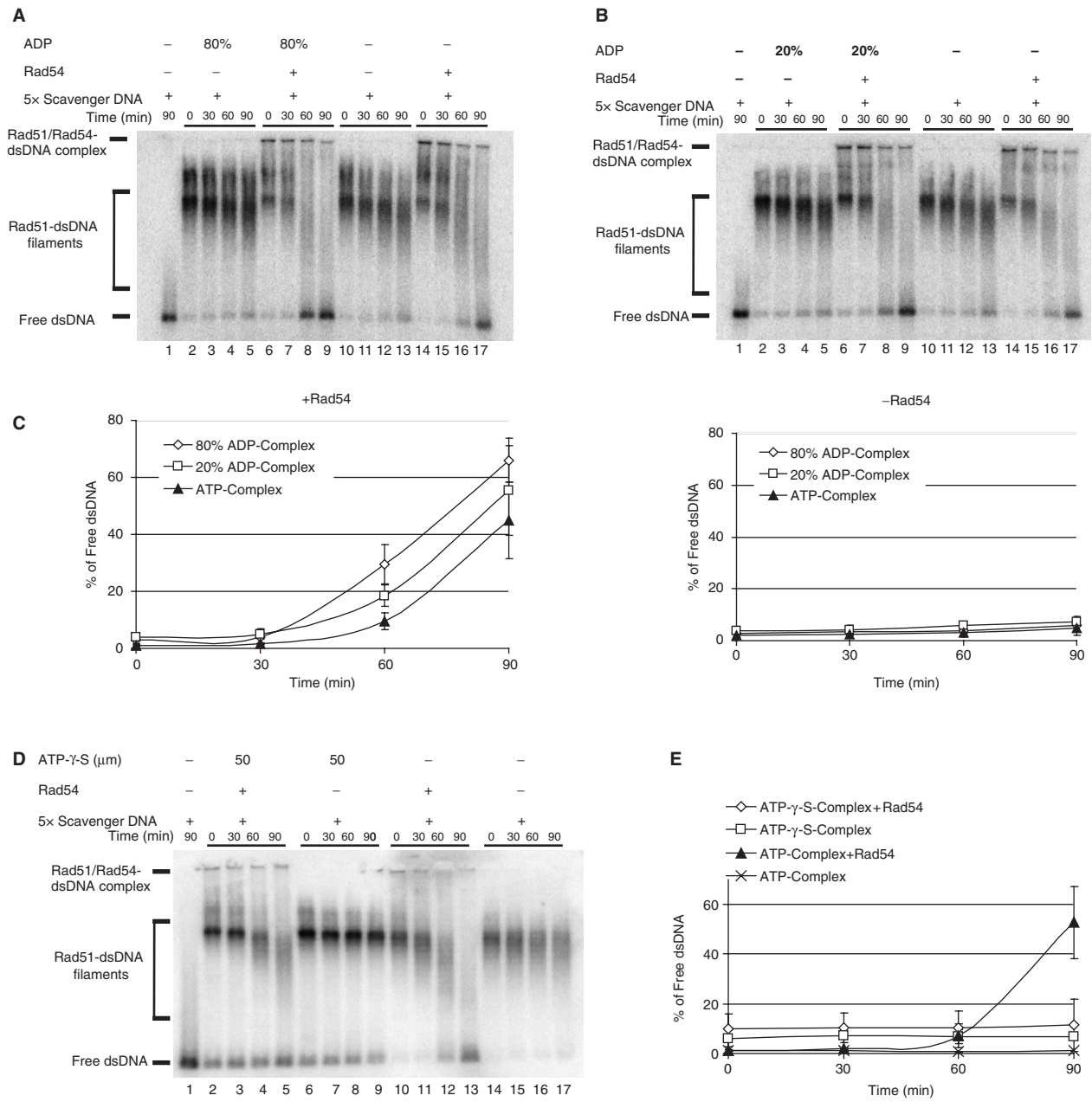

Figure 6. The effects of nucleotide cofactor on Rad51-dsDNA filament disassembly promoted by Rad54. (**A**) Rad51-dsDNA filaments were assembled at 4 bp/Rad51 (1.5 μM Rad51, 6 μM dsDNA) for 15 min at 30°C, either in the presence of 80% ADP (1 mM ATP and 4 mM ADP) or absence of ADP (5 mM ATP). Addition of Rad54 (50 nM) and scavenger DNA (30 μM) initiated the protein–DNA filament disassembly. Protein-free, labeled DNA substrate (lane 1); Rad51-dsDNA filaments in the absence of Rad54 but with ADP (lanes 2–5), in the presence of Rad54 and ADP (lanes 6–9), in the absence of Rad54 and ADP (lanes 10–13), in the presence of Rad54 but absence of ADP (lanes 14–17). (**B**) Rad51-dsDNA filaments were assembled as in (A) either in the presence of 20% ADP (4 mM ATP and 1 mM ADP) or absence of ADP (5 mM ATP). Addition of Rad54 (50 nM) and scavenger DNA (30 μM) initiated the protein–DNA filament disassembly. Protein-free, labeled DNA substrate (lane 1); Rad51-dsDNA filaments in the absence of Rad54 but with ADP (lanes 2–5), in the presence of Rad54 and ADP (lanes 6–9), in the absence of Rad54 and ADP (lanes 10–13), in the presence of Rad54 but absence of ADP (lanes 14–17). (**C**) The data from (A) and (B) were quantified on a PhosphoImager. The accumulation of free DNA was taken as readout of Rad51 displacement activity by Rad54. Data points represent the average of at least three replicate experiments and error bars represent one standard deviation. (**D**) Rad51-dsDNA filaments were assembled as in (A), either in the presence of ATP-γ-S (50 μM) or ATP (50 μM). Addition of Rad54 (50 nM), scavenger DNA (30 μM) and ATP (5 mM) initiates the protein–DNA filament disassembly. Protein-free, labeled DNA substrate (lane 1); Rad51-dsDNA filaments in the presence of Rad54 and ATP-γ-S (lanes 2–5), in the absence of Rad54 but with ATP-γ-S (lanes 6–9), in the presence of Rad54 but absence of ATP-γ-S (lanes 10–13), in the absence of Rad54 or ATP-γ-S (lanes 14–17). (**E**) The data from (D) were quantified on a PhosphoImager. The accumulation of the band of free DNA was taken as readout of Rad51 displacement activity by Rad54. Data points represent the average of at least three replicate experiments, and error bars represent 1 SD.

ADP-bound subunits displayed slower disappearance of the saturated complexes (Figure 6A, lanes 2–5, lanes 10–13; Figure 6B, lanes 2–5, lanes 10–13, Figure 6C). In these reactions, the ATP regeneration system was supplemented after filament assembly but before Rad54 addition to ensure optimal Rad54 activity. Control experiments confirmed that the Rad54 ATPase activity remained unaffected by the presence of ADP under these conditions (data not shown). Together, these results suggest that Rad54 prefers disassembling filaments containing Rad51 subunits bound to ADP. The observed effect represents a lower estimate as possible exchange of Rad51 bound ADP by ATP may occur under these reaction conditions.

If the low efficiency of Rad51-K191R-dsDNA filament disassembly by Rad54 is due to its ATPase defect (Figures 4 and 5), one prediction is that Rad51-dsDNA filaments assembled with the slowly hydrolysable ATP analog, ATP-γ-S, would have the same effect. Rad51-ATP-γ-S-dsDNA filaments were assembled in the presence of 50-μM ATP-γ-S. To initiate disassembly, Rad54 and 5-mM ATP were added together with the ATP regeneration system. Control ATPase assays showed that Rad54 maintained about 98% of its original ATPase activity under these conditions (data not shown). Compared with the nucleoprotein filament assembled with ATP, the Rad51-ATP-γ-S-dsDNA filament was only partially disassembled by Rad54 during the time course with no significant increase of protein-free DNA (Figure 6D, lanes 2–5, lanes 10–13, Figure 6E). In the absence of Rad54, filaments assembled with ATP-γ-S were extremely stable and resistant to the challenge by scavenger DNA (Figure 6D, lanes 6–9 and lanes 13–17). This is very reminiscent of the observation with the Rad51-K191R-ATP-dsDNA filaments (Figure 4C). In addition, in the presence of ATP-γ-S, Rad51 displayed a similar dsDNA-binding defect as the Rad51-K191R protein did with ATP, as indicated by the presence of free DNA (Figure 6D, lanes 2–9, Figure 6A). Taken together, these results support the idea that the Rad51-dsDNA filament formed in the presence of ATP-γ-S resembles the Rad51-K191R-ATP-dsDNA filament, and that intrinsic ATP hydrolysis by Rad51 is critical for its dissociation from dsDNA substrates. The resistance of the Rad51 filament to dissociation by Rad54 in the absence of Rad51 ATP hydrolysis is probably greater than observed here, because of residual ATP-γ-S hydrolysis and possible impurities in the ATP-γ-S preparation.

DISCUSSION

Rad51 and Rad54 are key DNA-dependent ATPases functioning in HR in eukaryotes. Our analysis uncovered unexpected biochemical properties of the ATPase-deficient Rad51-K191R and Rad51-K191A mutant proteins. Kinetic analysis and experiments with different nucleotide cofactors revealed an intricate relationship between the Rad51 and Rad54 ATPase activities, demonstrating that both ATPase activities are required for efficient turnover of the Rad51-dsDNA filament.

Biochemical properties of Rad51-K191A and Rad51-K191R proteins

The Walker A motif is a phosphate-binding loop that is found in many purine nucleotide-binding proteins including RecA and Rad51 (72). Mutations in the central lysine residue are often used to dissociate ATP binding and ATP hydrolysis, relying on an often untested assumption that the lysine to arginine substituted protein (e.g. Rad51-K191R) binds but does not hydrolyze ATP, whereas the lysine to alanine substituted protein (e.g. Rad51-K191A) cannot bind ATP. Surprisingly, we find that both Rad51-K191R and Rad51-K191A mutant proteins bind ATP, albeit with reduced affinity compared with the wild-type protein (Table 1). Both mutant proteins bound DNA in a nucleotide-dependent manner (Figure 2; data not shown). However, only the Rad51-K191R protein formed filaments that displayed DNA strand invasion activity and normal stimulation of Rad54 ATPase activity [Table 3 and data not shown; (14,44)]. Whereas, the Rad51-K191A-DNA complexes were non-functional and defective in stimulating Rad54 ATPase activity or promoting strand invasion [data not shown; (44)]. These biochemical data are consistent with *in vivo* observations that determined that the budding yeast *rad51-K191A* is phenotypically null (20). Also the human Rad51-K133A protein was found to bind ATP (also with lower affinity) (28), confirming our observation that this amino acid change in the Walker A box does not always eliminate ATP binding.

Unexpectedly, Rad51-K191R displayed a DNA binding defect that is revealed by a requirement for higher protein concentrations to form DNA complexes (Figure 2A) and by lower STMs in the formation of protein DNA complexes (73). The nucleoprotein gel analysis showed that Rad51-K191R protein formed fewer complexes with intermediate electrophoretic mobility, which could be a reflection of a nucleation defect or of increased cooperativity. Rad51 is known to display significantly lower cooperativity than RecA protein (61). These results demonstrate a reduced affinity for DNA (Figure 2, Table 2), consistent with data from single-molecule experiments using the human Rad51-K133R protein and phage λ dsDNA (74). Importantly, ATP hydrolysis appears to be critical for the dynamic turnover of the Rad51-ssDNA and dsDNA filaments, since the filaments formed by the Rad51-K191R protein were significantly more stable than filaments formed by wild-type Rad51 protein. These results are consistent with previous observations made with the human Rad51 protein (15,16). Furthermore, our results show that the stability of the Rad51-K191R-dsDNA complexes is significantly more pronounced than that of the ssDNA complexes.

Together, these results suggest that the *rad51-K191R* mutant *in vivo* may lead to defects in presynapsis, in Rad51-ssDNA filament formation, and in postsynapsis, in Rad51-dsDNA filament dissociation. This interpretation of the biochemical data is supported by genetic analysis (20,73). Overexpression of Rad51-K191R and deletion of the *SRS2* gene were found to suppress the *rad51-K191R* defect (20,73). Since Srs2 is only able to

dissociate Rad51 from ssDNA (75,76), these findings support a defect of Rad51-K191R during presynapsis. It is not possible to distinguish whether this is due to decreased ATP binding, which may be the root cause for the DNA binding defect, or to the greatly reduced dynamics of the filament due to the higher stability of the Rad51-K191R-ssDNA filaments. On the other hand, overexpression of Rad54 also suppressed the *rad51-K191R* defect (20). Since Rad54 can only dissociate Rad51 from dsDNA, these data suggest that the Rad51 ATPase activity is also required *in vivo* for turnover from dsDNA. Overexpression of Rad54 may also suppress a potential presynaptic defect by possibly enhancing the non-DNA bound Rad51 pool. Dissociation of dead-end complexes of Dmc1 and dsDNA appears to be a critical function for the Rdh54/Tid1 protein, which is closely related to Rad54 (77).

Rad54 ATPase

The Rad54 ATPase activity exhibits a basic mode of protein-free dsDNA, a filament mode with reduced ATPase activity on fully saturated Rad51-dsDNA filaments, and an enhanced mode on sub-saturated Rad51-dsDNA filaments (61). Here, we provide kinetic data to distinguish these three modes. Stimulation of Rad54 ATPase activity on partial Rad51-dsDNA filaments compared with protein-free DNA is specifically due to an increase in the V_{MAX} for ATP enhancing the catalytic efficiency about 6-fold with no significant change in the K_M for ATP (Table 3). In contrast, with saturated Rad51-dsDNA filament, the V_{MAX} for ATP is reduced to about 70% coupled with a significant increase in affinity for ATP indicated by a 15-fold lower K_M for ATP (Table 3) when compared with protein-free DNA. These data suggest that Rad54 undergoes a conformational change from a high K_M form that can translocate on DNA (protein-free DNA, partial Rad51-dsDNA filament) to a low K_M form when associated with fully saturated Rad51-DNA filaments. Rad54 is a bi-directional, processive motor protein on dsDNA (31). This property is reminiscent of the FtsK motor protein, which forms a double-hexameric ring on dsDNA for translocation (78). While the precise assembly of the translocating and non-translocating Rad54 protein remains to be determined, electron microscopic analysis of negatively stained specimens identified a Rad54 oligomeric assembly on protein-free dsDNA and dsDNA partially saturated by Rad51 protein (62), which is consistent with this hypothesis.

The K_M (ATP) of Rad54 on protein-free dsDNA that we determined in our experiments is about 6–7-fold higher than that measured by Amitani *et al.* (31) in single-molecule experiments. We ascertained our high K_M in experiments using a different concentration of Rad54 (9 nM instead of 3.3 nM; data not shown). We observe that Rad54 ATPase activities (Figure 3A) with protein-free and partial Rad51-dsDNA filaments very gradually approached the saturation point with only minor increases in ATPase activity above 1 mM, whereas the ATPase activity with fully saturated filaments (Figure 3B) approach saturation more rapidly with no increase above 1 mM. Our K_M determination is based on ATPase activity as an output, whereas Amitani *et al.* (31) measured translocation velocity, detecting no increase in velocity above 0.5 mM (31). It is possible that the low K_M determined in the translocation experiments reflects the ATP-binding of the DNA-bound subunit of an oligomeric assembly. In our ATPase experiments, the minor increase in ATPase activity at high ATP concentrations may reflect ATP binding of the non-DNA bound subunits. Consistent with this interpretation, our Rad54 K_M data measuring ATPase activity with fully saturated Rad51-dsDNA filaments (Table 3), where Rad54 is likely in a non-translocating oligomeric state, are essentially identical with the K_M determined by velocity in the translocation experiments on protein-free DNA (31).

Differences between RecA, yeast Rad51 and human Rad51

Despite their evolutionary conservation, significant differences exist between RecA, yeast Rad51 and human Rad51 with respect to their ATPase activity and DNA binding properties. RecA autonomously toggles between a high affinity (ATP) and low affinity binding state (ADP) by nucleotide cofactor binding and cooperative hydrolysis, resulting in dynamic assembly and turnover of RecA filaments (79). Unlike RecA (and human Rad51), yeast Rad51 binding to DNA depends on the presence of nucleotide cofactor at neutral pH (70). The significantly lower (~200-fold) and non-cooperative ATPase activity of Rad51 (10) results in a far less dynamic filament. Also unlike RecA, which has a kinetic impediment to bind dsDNA, yeast and human Rad51 readily bind dsDNA (70). Human Rad51 resembles more RecA than yeast Rad51 in its ability to bind DNA independent of nucleotide co-factor, but shares the low and non-cooperative ATPase activity with its yeast counterpart (15,28,80,81). Likely as a consequence, Rad51-DNA complexes are much more stable and less dynamic than RecA filaments [(15,16) and this study]. Rad51 binding to dsDNA and the relative stability of these complexes will lead to dead-end complexes on undamaged DNA. Moreover, Rad51 is stuck on the heteroduplex DNA product after DNA strand exchange. We have previously proposed that a major role of Rad54 is to function as an extrinsic turnover factor for the Rad51-dsDNA filament, suggesting that the combination of Rad51 and Rad54 reflect the eukaryotic equivalent of RecA in recombination (41,61).

Role of the Rad51 and Rad54 ATPase activities in the turnover of Rad51-dsDNA filaments

Previously we established that the Rad54 motor activity was required for Rad51 dissociation from dsDNA (41,61). Here, we show that both the Rad51 and Rad54 ATPase activities are required for efficient turnover of the Rad51-dsDNA complex. The reduced dissociation efficiency of Rad51-K191R-dsDNA filaments by Rad54 appears to be a direct consequence of the ATP hydrolysis defect by Rad51-K191R protein. To rule out an unrelated defect of this protein, we assembled wild-type Rad51-dsDNA filaments in the presence of ATP-γ-S, a very slowly hydrolyzable ATP analog, and showed a similar turnover

defect as with Rad51-K191R-dsDNA filaments. This demonstrates that the Rad51-dsDNA filament is not a passive remodeling substrate for the Rad54 motor, but that both ATPase activities modulate Rad51-dsDNA filament dynamics.

Since ATP hydrolysis is closely associated with the disassembly of the Rad51-dsDNA complex, the nucleotide factors bound to Rad51 may act as a signal that determines the dynamic state of the nucleoprotein filament. It is well known in actin filaments and microtubules that ATP-bound subunits associate at one end and ADP-bound subunits dissociate from the other end, leading to a treadmilling of subunits in the steady state (82,83). A similar model has been proposed for RecA filaments (79). When Rad51-dsDNA filaments were formed in the presence of ADP, spontaneous disassembly appeared unchanged. However, in the presence of Rad54 the ADP-containing filaments were dissociated more efficiently in an ADP concentration-dependent manner (Figures 6A, B and C). Hence, Rad51-ADP-dsDNA complexes are better substrates for Rad54, suggesting that the Rad54 motor may have a preference for binding to the ADP-bound end compared with the ATP-bound end. This interpretation is consistent with electron microscopic observations, showing an overabundance of Rad54 particles associated with a single end of the Rad51-dsDNA filament (62). It is also possible that Rad54 dissociates an ATP-bound terminal subunit that leads to faster dissociation of ADP-containing Rad51 filaments. During recombination, Rad54 is targeted to the pairing site by its interaction with the Rad51-ssDNA filament (46), possibly orienting the motor to the ADP-Rad51 end of the Rad51-dsDNA product complex to aid in Rad51 dissociation from dsDNA. Regulation of the dynamic state of the Rad51-dsDNA filament is likely of biological significance. It not only allows recycling of Rad51, but also coordinates the transition to downstream events in the HR pathway, in particular the access of DNA polymerases to the invading 3′ end.

ACKNOWLEDGEMENTS

We thank Steve Kowalczykowski for his insightful comments and for sharing his instruments, Lorraine Symington for sharing unpublished results and her valuable comments, and Shannon Ceballos, Tony Forget, Kristina Herzberg, Eugene Nadezhdin, Erin Schwartz and William Wright for their helpful criticism of the manuscript. This work was supported by NIH grants GM58015 (to W.-D.H.) and GM35269 (to E.H.E.) and a Susan G. Komen Breast Cancer Foundation postdoctoral fellowship PDF403213 (to XPZ). Funding to pay the Open Access publication charges for this article was provided by NIH grant GM58015.

Conflict of interest statement. None declared.

REFERENCES

1. Krogh,B.O. and Symington,L.S. (2004) Recombination proteins in yeast. *Annu. Rev. Genet.*, **38**, 233–271.
2. Paques,F. and Haber,J.E. (1999) Multiple pathways of recombination induced by double-strand breaks in *Saccharomyces cerevisiae*. *Microbiol. Mol. Biol. Rev.*, **63**, 349–404.
3. Dronkert,M.L.G. and Kanaar,R. (2001) Repair of DNA interstrand cross-links. *Mutat. Res. DNA Repair*, **486**, 217–247.
4. Kowalczykowski,S.C. (2000) Initiation of genetic recombination and recombination-dependent replication. *Trends Biochem. Sci.*, **25**, 156–165.
5. Kolodner,R.D., Putnam,C.D. and Myung,K. (2002) Maintenance of genome stability in *Saccharomyces cerevisiae*. *Science*, **297**, 552–557.
6. New,J.H., Sugiyama,T., Zaitseva,E. and Kowalczykowski,S.C. (1998) Rad52 protein stimulates DNA strand exchange by Rad51 and replication protein A. *Nature*, **391**, 407–410.
7. Sung,P. (1997) Yeast Rad55 and Rad57 proteins form a heterodimer that functions with replication protein A to promote DNA strand exchange by Rad51 recombinase. *Genes Dev.*, **11**, 1111–1121.
8. Sung,P. (1997) Function of yeast Rad52 protein as a mediator between replication protein A and the Rad51 recombinase. *J. Biol. Chem.*, **272**, 28194–28197.
9. Shinohara,A. and Ogawa,T. (1998) Stimulation by Rad52 of yeast Rad51-mediated recombination. *Nature*, **391**, 404–407.
10. Sung,P. (1994) Catalysis of ATP-dependent homologous DNA pairing and strand exchange by yeast RAD51 protein. *Science*, **265**, 1241–1243.
11. Ogawa,T., Yu,X., Shinohara,A. and Egelman,E.H. (1993) Similarity of the yeast RAD51 filament to the bacterial RecA filament. *Science*, **259**, 1896–1899.
12. Shinohara,A., Ogawa,H. and Ogawa,T. (1992) Rad51 protein involved in repair and recombination in *S. cerevisiae* is a RecA-like protein. *Cell*, **69**, 457–470.
13. Aboussekhra,A., Chanet,R., Adjiri,A. and Fabre,F. (1992) Semi-dominant suppressors of Srs2 helicase mutations of *Saccharomyces cerevisiae* map in the *RAD51* gene, whose sequence predicts a protein with similarities to procaryotic RecA protein. *Mol. Cell. Biol.*, **12**, 3224–3234.
14. Sung,P. and Stratton,S.A. (1996) Yeast Rad51 recombinase mediates polar DNA strand exchange in the absence of ATP hydrolysis. *J. Biol. Chem.*, **271**, 27983–27986.
15. Chi,P., Van Komen,S., Sehorn,M.G., Sigurdsson,S. and Sung,P. (2006) Roles of ATP binding and ATP hydrolysis in human Rad51 recombinase function. *DNA Repair*, **5**, 381–391.
16. Ristic,D., Modesti,M., van der Heijden,T., van Noort,J., Dekker,C., Kanaar,R. and Wyman,C. (2005) Human Rad51 filaments on double- and single-stranded DNA: correlating regular and irregular forms with recombination function. 33, 3292–3302.
17. Rehrauer,W.M. and Kowalczykowski,S.C. (1993) Alteration of the Nucleoside Triphosphate (NTP) Catalytic Domain Within Escherichia-Coli recA Protein Attenuates NTP Hydrolysis But Not Joint Molecule Formation. *J. Biol. Chem.*, **268**, 1292–1297.
18. Shan,Q., Cox,M.M. and Inman,R.B. (1996) DNA strand exchange promoted by RecA K72R - Two reaction phases with different Mg2+ requirements. *J. Biol. Chem.*, **271**, 5712–5724.
19. Rosselli,W. and Stasiak,A. (1990) Energetics of RecA-mediated recombination reactions. *J. Mol. Biol.*, **216**, 335–352.
20. Morgan,E.A., Shah,N. and Symington,L.S. (2002) The requirement for ATP hydrolysis by Saccharomyces cerevisiae Rad51 is bypassed by mating-type heterozygosity or RAD54 in high copy. *Mol. Cell. Biol.*, **22**, 6336–6343.
21. Konola,J.T., Logan,K.M. and Knight,K.L. (1994) Functional Characterization of Residues in the P-Loop Motif of the RecA Protein ATP Binding Site. *J. Mol. Biol.*, **237**, 20–34.
22. Logan,K.M. and Knight,K.L. (1993) Mutagenesis of the P-Loop Motif in the ATP Binding Site of the RecA Protein from Escherichia-coli. *J. Mol. Biol.*, **232**, 1048–1059.
23. Campbell,M.J. and Davis,R.W. (1999) On the in vivo function of the RecA ATPase. *J. Mol. Biol.*, **286**, 437–445.
24. Campbell,M.J. and Davis,R.W. (1999) Toxic mutations in the recA gene of E. coli prevent proper chromosome segregation. *J. Mol. Biol.*, **286**, 417–435.
25. Stark,J.M., Pierce,A.J., Oh,J., Pastink,A. and Jasin,M. (2004) Genetic steps of mammalian homologous repair with distinct mutagenic consequences. *Mol. Cell. Biol.*, **24**, 9305–9316.

26. Stark,J.M., Hu,P., Pierce,A.J., Moynahan,M.E., Ellis,N. and Jasin,M. (2002) ATP hydrolysis by mammalian RAD51 has a key role during homology-directed DNA repair. *J. Biol. Chem.*, **277**, 20185–20194.
27. Morrison,C., Shinohara,A., Sonoda,E., Yamaguchi-Iwai,Y., Takata,M., Weichselbaum,R. and Takeda,S. (1999) The essential functions of human Rad51 are independent of ATP-hydrolysis. *Mol. Cell. Biol.*, **19**, 6891–6897.
28. Forget,A.L., Loftus,M.S., McGrew,D.A., Bennett,B.T. and Knight,K.L. (2007) The Human Rad51 K133A Mutant Is Functional for DNA Double-Strand Break Repair in Human Cells. *Biochemistry*, **46**, 3566–3575.
29. Tan,T.L.R., Kanaar,R. and Wyman,C. (2003) Rad54, a Jack of all trades in homologous recombination. *DNA Repair*, **2**, 787–794.
30. Heyer,W.D., Li,X., Rolfsmeier,M. and Zhang,X.P. (2006) Rad54: the Swiss Army knife of homologous recombination? *Nucleic Acids Res.*, **34**, 4115–4125.
31. Amitani,I., Baskin,R.J. and Kowalczykowski,S.C. (2006) Visualization of Rad54, a chromatin remodeling protein, translocating on single DNA molecules. *Mol. Cell*, **23**, 143–148.
32. Schmuckli-Maurer,J., Rolfsmeier,M., Nguyen,H. and Heyer,W.-D. (2003) Genome instability in *RAD54* mutants of *Saccharomyces cerevisiae*. *Nucleic Acids Res.*, **31**, 1013–1023.
33. Clever,B., Schmuckli-Maurer,J., Sigrist,M., Glassner,B. and Heyer,W.-D. (1999) Specific negative effects resulting from elevated levels of the recombinational repair protein Rad54p in *Saccharomyces cerevisiae*. *Yeast*, **15**, 721–740.
34. Petukhova,G., Van Komen,S., Vergano,S., Klein,H. and Sung,P. (1999) Yeast Rad54 promotes Rad51-dependent homologous DNA pairing via ATP hydrolysis-driven change in DNA double helix conformation. *J. Biol. Chem.*, **274**, 29453–29462.
35. Solinger,J.A., Lutz,G., Sugiyama,T., Kowalczykowski,S.C. and Heyer,W.-D. (2001) Rad54 protein stimulates heteroduplex DNA formation in the synaptic phase of DNA strand exchange via specific interactions with the presynaptic Rad51 nucleoprotein filament. *J. Mol. Biol.*, **307**, 1207–1221.
36. Swagemakers,S.M.A., Essers,J., deWit,J., Hoeijmakers,J.H.J. and Kanaar,R. (1998) The human Rad54 recombinational DNA repair protein is a double-stranded DNA-dependent ATPase. *J. Biol. Chem.*, **273**, 28292–28297.
37. Clever,B., Interthal,H., Schmuckli-Maurer,J., King,J., Sigrist,M. and Heyer,W.D. (1997) Recombinational repair in yeast: Functional interactions between Rad51 and Rad54 proteins. *EMBO J.*, **16**, 2535–2544.
38. Jiang,H., Xie,Y.Q., Houston,P., Stemke-Hale,K., Mortensen,U.H., Rothstein,R. and Kodadek,T. (1996) Direct association between the yeast Rad51 and Rad54 recombination proteins. *J. Biol. Chem.*, **271**, 33181–33186.
39. Golub,E.I., Kovalenko,O.V., Gupta,R.C., Ward,D.C. and Radding,C.M. (1997) Interaction of human recombination proteins Rad51 and Rad54. *Nucleic Acids Res.*, **25**, 4106–4110.
40. Mazin,A.V., Alexeev,A.A. and Kowalczykowski,S.C. (2003) A novel function of Rad54 protein - Stabilization of the Rad51 nucleoprotein filament. *J. Biol. Chem.*, **278**, 14029–14036.
41. Solinger,J.A., Kiianitsa,K. and Heyer,W.-D. (2002) Rad54, a Swi2/Snf2-like recombinational repair protein, disassembles Rad51:dsDNA filaments. *Mol. Cell*, **10**, 1175–1188.
42. Wolner,B. and Peterson,C.L. (2005) ATP-dependent and ATP-independent roles for the Rad54 chromatin remodeling enzyme during recombinational repair of a DNA double strand break. *J. Biol. Chem.*, **280**, 10855–10860.
43. Petukhova,G., Stratton,S. and Sung,P. (1998) Catalysis of homologous DNA pairing by yeast Rad51 and Rad54 proteins. *Nature*, **393**, 91–94.
44. Van Komen,S., Petukhova,G., Sigurdsson,S., Stratton,S. and Sung,P. (2000) Superhelicity-driven homologous DNA pairing by yeast recombination factors Rad51 and Rad54. *Mol. Cell*, **6**, 563–572.
45. Sigurdsson,S., Van Komen,S., Petukhova,G. and Sung,P. (2002) Homologous DNA pairing by human recombination factors Rad51 and Rad54. *J. Biol. Chem.*, **277**, 42790–42794.
46. Mazin,A.V., Bornarth,C.J., Solinger,J.A., Heyer,W.-D. and Kowalczykowski,S.C. (2000) Rad54 protein is targeted to pairing loci by the Rad51 nucleoprotein filament. *Mol. Cell*, **6**, 583–592.
47. Alexeev,A., Mazin,A. and Kowalczykowski,S.C. (2003) Rad54 protein possesses chromatin-remodeling activity stimulated by a Rad51-ssDNA nucleoprotein filament. *Nat. Struct. Biol.*, **10**, 182–186.
48. Jaskelioff,M., Van Komen,S., Krebs,J.E., Sung,P. and Peterson,C.L. (2003) Rad54p is a chromatin remodeling enzyme required for heteroduplex joint formation with chromatin. *J. Biol. Chem.*, **278**, 9212–9218.
49. Alexiadis,V. and Kadonaga,J.T. (2003) Strand pairing by Rad54 and Rad51 is enhanced by chromatin. *Genes Dev.*, **16**, 2767–2771.
50. Solinger,J.A. and Heyer,W.-D. (2001) Rad54 protein stimulates the postsynaptic phase of Rad51 protein-mediated DNA strand exchange. *Proc. Natl Acad. Sci. USA*, **98**, 8447–8453.
51. Bugreev,D.V., Mazina,O.M. and Mazin,A.V. (2006) Rad54 protein promotes branch migration of Holliday junctions. *Nature*, **442**, 590–593.
52. West,S.C. (1996) The RuvABC proteins and Holliday junction processing in *Escherichia coli*. *J. Bacteriol.*, **178**, 1237–1241.
53. Kim,P.M., Paffett,K.S., Solinger,J.A., Heyer,W.D. and Nickoloff,J.A. (2002) Spontaneous and double-strand break-induced recombination, and gene conversion tract lengths, are differentially affected by overexpression of wild-type or ATPase-defective yeast Rad54. *Nucleic Acids Res.*, **30**, 2727–2735.
54. Rattray,A.J. and Symington,L.S. (1995) Multiple pathways for homologous recombination in *Saccharomyces cerevisiae*. *Genetics*, **139**, 45–56.
55. Shinohara,M., Gasior,S.L., Bishop,D.K. and Shinohara,A. (2000) Tid1/Rdh54 promotes colocalization of Rad51 and Dmc1 during meiotic recombination. *Proc. Natl Acad. Sci. USA*, **97**, 10814–10819.
56. Miyazaki,T., Bressan,D.A., Shinohara,M., Haber,J.E. and Shinohara,A. (2004) *In vivo* assembly and disassembly of Rad51 and Rad52 complexes during double-strand break repair. *EMBO J.*, **23**, 939–949.
57. Takata,M., Sasaki,M.S., Sonoda,E., Fukushima,T., Morrison,C., Albala,J.S., Swagemakers,S.M.A., Kanaar,R., Thompson,L.H. *et al.* (2000) The Rad51 paralog Rad51B promotes homologous recombinational repair. *Mol. Cell. Biol.*, **20**, 6476–6482.
58. Wesoly,J., Agarwal,S., Sigurdsson,S., Bussen,W., Van Komen,S., Qin,J.A., van Steeg,H., van Benthem,J., Wassenaar,E. *et al.* (2006) Differential contributions of mammalian Rad54 paralogs to recombination, DNA damage repair, and meiosis. *Mol. Cell. Biol.*, **26**, 976–989.
59. Wolner,B., van Komen,S., Sung,P. and Peterson,C.L. (2003) Recruitment of the recombinational repair machinery to a DNA double-strand break in yeast. *Mol. Cell*, **12**, 221–232.
60. Sugawara,N., Wang,X. and Haber,J.E. (2003) *In vivo* roles of Rad52, Rad54, and Rad55 proteins in Rad51-mediated recombination. *Mol. Cell*, **12**, 209–219.
61. Kiianitsa,K., Solinger,J.A. and Heyer,W.D. (2002) Rad54 protein exerts diverse modes of ATPase activity on duplex DNA partially and fully covered with Rad51 protein. *J. Biol. Chem.*, **277**, 46205–46215.
62. Kiianitsa,K., Solinger,J.A. and Heyer,W.D. (2006) Terminal association of Rad54 protein with the Rad51-dsDNA filament. *Proc. Natl Acad. Sci. USA*, **103**, 9767–9772.
63. Walker,P.A., Leong,L.E., Ng,P.W., Tan,S.H., Waller,S., Murphy,D. and Porter,A.G. (1994) Efficient and rapid affinity purification of proteins using recombinant fusion proteases. *Biotechnology (NY)*, **12**, 601–605.
64. Kiianitsa,K., Solinger,J.A. and Heyer,W-D. (2003) NADH-coupled microplate photometric assay for kinetic studies of ATP-hydrolyzing enzymes with low and high specific activities. *Anal. Biochem.*, **321**, 266–271.
65. Sung,P., Higgins,D., Prakash,L. and Prakash,S. (1988) Mutation of lysine-48 to arginine in the yeast RAD3 protein abolishes its ATPase and DNA helicase activities but not the ability to bind ATP. *EMBO J.*, **7**, 3263–3269.
66. Tombline,G., Shim,K.S. and Fishel,R. (2002) Biochemical characterization of the human RAD51 protein - II. Adenosine nucleotide binding and competition. *J. Biol. Chem.*, **277**, 14426–14433.

67. Potter,R.L. and Haley,B.E. (1983) Photoaffinity labeling of nucleotide binding sites with 8-azidopurine analogs: techniques and applications. *Methods Enzymol.*, **91**, 613–633.
68. Dunn,K., Chrysogelos,S. and Griffith,J. (1982) Electron microscopic visualization of recA-DNA filaments: evidence for a cyclic extension of duplex DNA. *Cell*, **28**, 757–765.
69. Liu,Y.L., Stasiak,A.Z., McLlwraith,M.J., Stasiak,A. and West,S.C. (2004) Conformational changes modulate the activity of human RAD51 protein. *J. Mol. Biol.*, **337**, 817–827.
70. Zaitseva,E.M., Zaitsev,E.N. and Kowalczykowski,S.C. (1999) The DNA binding properties of *Saccharomyces cerevisiae* Rad51 protein. *J. Biol. Chem.*, **274**, 2907–2915.
71. Record,M.T. Jr, Lohman,M.L. and De Haseth,P. (1976) Ion effects on ligand-nucleic acid interactions. *J. Mol. Biol.*, **107**, 145–158.
72. Walker,J.E., Saraste,M., Runswick,M.J. and Gay,N.J. (1982) Distantly related sequences in the a- and b-subunits of ATP synthase, myosin, kinases and other ATP-requiring enzymes and a common nucleotide binding fold. *EMBO J.*, **1**, 945–951.
73. Fung,C.W., Fortin,G.S., Peterson,S.E. and Symington,L.S. (2006) The rad51-K191R ATPase-defective mutant is impaired for presynaptic filament formation. *Mol. Cell. Biol.*, **26**, 9544–9554.
74. Prasad,T.K., Yeykal,C.C. and Greene,E.C. (2006) Visualizing the Assembly of Human Rad51 Filaments on Double-stranded DNA. *J. Mol. Biol.*, **363**, 713–728.
75. Krejci,L., Van Komen,S., Li,Y., Villemain,J., Reddy,M.S., Klein,H., Ellenberger,T. and Sung,P. (2003) DNA helicase Srs2 disrupts the Rad51 presynaptic filament. *Nature*, **423**, 305–309.
76. Veaute,X., Jeusset,J., Soustelle,C., Kowalczykowski,S.C., Le Cam,E. and Fabre,F. (2003) The Srs2 helicase prevents recombination by disrupting Rad51 nucleoprotein filaments. *Nature*, **423**, 309–312.
77. Holzen,T.M., Shah,P.P., Olivares,H.A. and Bishop,D.K. (2006) Tid1/Rdh54 promotes dissociation of Dmc1 from nonrecombinogenic sites on meiotic chromatin. *Genes Dev.*, **20**, 2593–2604.
78. Massey,T.H., Mercogliano,C.P., Yates,J., Sherratt,D.J. and Lowe,J. (2006) Double-stranded DNA translocation: structure and mechanism of hexameric FtsK. *Mol. Cell*, **23**, 457–469.
79. Kowalczykowski,S.C. (1991) Biochemistry of genetic recombination: energetics and mechanism of DNA strand exchange. *Annu. Rev. Biophys. Biophys. Chem.*, **20**, 539–575.
80. Tombline,G., Heinen,C.D., Shim,K.S. and Fishel,R. (2002) Biochemical characterization of the human RAD51 protein - III. - Modulation of DNA binding by adenosine nucleotides. *J. Biol. Chem.*, **277**, 14434–14442.
81. De Zutter,J.K. and Knight,K.L. (1999) The hRad51 and RecA proteins show significant differences in cooperative binding to sing;e-stranded DNA. *J. Mol. Biol.*, **293**, 769–780.
82. Pollard,T.D. and Borisy,G.G. (2003) Cellular motility driven by assembly and disassembly of actin filaments. *Cell*, **112**, 453–465.
83. Moritz,M. and Agard,D.A. (2001) Gamma-tubulin complexes and microtubule nucleation. *Curr. Opin. Struct. Biol.*, **11**, 174–181.